AD-A078 775 COLD REGIONS RESEARCH AND ENGINEERING LAB HANOVER NH F/G 8/12
CHARGED DISLOCATION IN ICE. I. EXISTENCE AND CHARGE DENSITY MEA--ETC(U)
NOV 79 K ITAGAKI

UNCLASSIFIED CRREL-79-25 NL

| OF |
AD
A078775

END
DATE
FILMED
1 80
DDC

CRREL

REPORT 79-25

LEVEL

Charged dislocation in ice

I. Existence and charge density measurement by X-ray topography

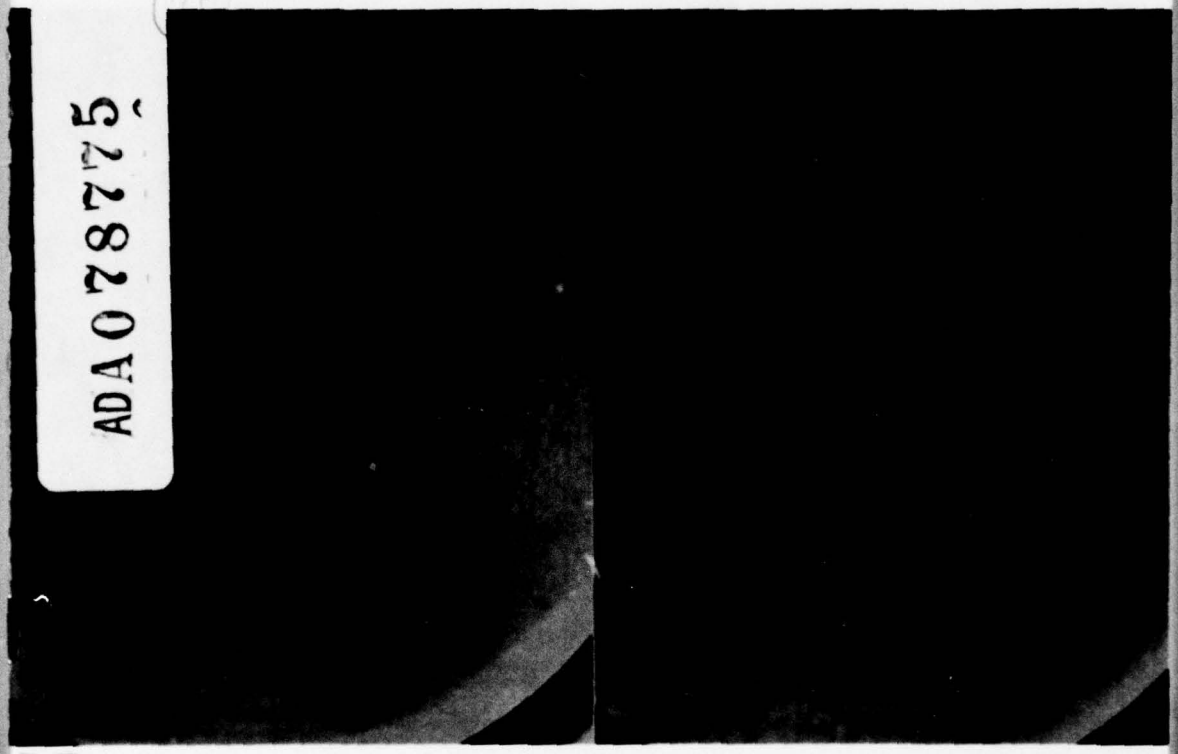

$$A\frac{\partial^2\eta}{\partial t^2} + B\frac{\partial\eta}{\partial t} - C\frac{\partial^2\eta}{\partial x^2} = E'\mu e^{i\omega t}$$

For conversion of SI metric units to U.S./British customary units of measurement consult ASTM Standard E380, Metric Practice Guide, published by the American Society for Testing and Materials, 1916 Race St., Philadelphia, Pa. 19103.

Cover: Comparison of dislocation image without (left) and with an electric field of 32,000 V/m. (Photographs by K. Itagaki.)

CRREL Report 79-25

Charged dislocation in ice

I. Existence and charge density measurement by X-ray topography

Kazuhiko Itagaki

November 1979

Prepared for
DIRECTORATE OF MILITARY PROGRAMS
OFFICE, CHIEF OF ENGINEERS
By
UNITED STATES ARMY
CORPS OF ENGINEERS
COLD REGIONS RESEARCH AND ENGINEERING LABORATORY
HANOVER, NEW HAMPSHIRE, U.S.A.

Unclassified

SECURITY CLASSIFICATION OF THIS PAGE (When Data Entered)

REPORT DOCUMENTATION PAGE

READ INSTRUCTIONS BEFORE COMPLETING FORM

1. REPORT NUMBER: CRREL [illegible]9-25
2. GOVT ACCESSION NO.
3. RECIPIENT'S CATALOG NUMBER

4. TITLE (and Subtitle): CHARGED DISLOCATION IN ICE: I. EXISTENCE AND CHARGE DENSITY MEASUREMENT BY X-RAY TOPOGRAPHY
5. TYPE OF REPORT & PERIOD COVERED
6. PERFORMING ORG. REPORT NUMBER

7. AUTHOR(s): Kazuhiko Itagaki
8. CONTRACT OR GRANT NUMBER(s)

9. PERFORMING ORGANIZATION NAME AND ADDRESS: U.S. Army Cold Regions Research and Engineering Laboratory, Hanover, New Hampshire 03755
10. PROGRAM ELEMENT, PROJECT, TASK AREA & WORK UNIT NUMBERS: DA Project 4A161102AT24, Task C, Work Unit 002

11. CONTROLLING OFFICE NAME AND ADDRESS: Directorate of Military Programs, Office, Chief of Engineers, Washington, D.C. 20314
12. REPORT DATE: Nov[illegible]979
13. NUMBER OF PAGES: 14

14. MONITORING AGENCY NAME & ADDRESS (if different from Controlling Office)
15. SECURITY CLASS. (of this report): Unclassified
15a. DECLASSIFICATION/DOWNGRADING SCHEDULE

16. DISTRIBUTION STATEMENT (of this Report)

Approved for public release; distribution unlimited.

17. DISTRIBUTION STATEMENT (of the abstract entered in Block 20, if different from Report)

18. SUPPLEMENTARY NOTES

19. KEY WORDS (Continue on reverse side if necessary and identify by block number)

Dislocations
Electric charge
Ice
Single crystals
Topography
X-rays

20. ABSTRACT (Continue on reverse side if necessary and identify by block number)

The motion of dislocations in single crystal ice under an electric field was observed by using X-ray topographic methods. Electric charge density on these dislocations was deduced from the amplitude and length of the dislocation segment under the known AC electrical field. The most likely linear charge density was about $+5 \times 10^{-11}$ C/m, although considerable variation is possible depending on the effective field acting on the dislocation lines.

+5 x 10 to the minus 11th power C/m

DD FORM 1 JAN 73 1473 EDITION OF 1 NOV 65 IS OBSOLETE

037100

Unclassified

SECURITY CLASSIFICATION OF THIS PAGE (When Data Entered)

PREFACE

This report was prepared by Dr. Kazuhiko Itagaki, Research Physicist, of the Snow and Ice Branch, Research Division, U.S. Army Cold Regions Research and Engineering Laboratory. Funding for this research was provided by DA Project 4A161102AT24, *Research in Snow, Ice and Frozen Ground*, Task C, *Research in Terrain and Climatic Constraints*, Work Unit 002, *Adhesion and Physics of Ice*.

The author wishes to thank Stephen Ackley and Dr. Steven Arcone for technically reviewing the manuscript of this report and K.W. Kawate for checking the local field calculations.

CONTENTS

ILLUSTRATIONS

TABLES

CHARGED DISLOCATION IN ICE

I. Existence and Charge Density Measurement by X-ray Topography

Kazuhiko Itagaki

INTRODUCTION

Extensive studies on electrically charged dislocations in ionic crystals have been made. A review by Whitworth (1975) covered a wide range of topics concerning charged dislocation processes; however, little consideration has been given to the possible effect of mobile charged dislocations on dielectric polarization.

There are several investigations (Sproull 1960, Zagoruiko 1965, Turner and Whitworth 1968) indicating that the charged dislocations can be displaced by an electric field applied to a crystal. The additional polarization caused by the displaced charged dislocations can contribute to some of the dielectric relaxation spectra. A brief discussion of the contribution to dielectric relaxation and the possible effect of deformation was given by the present author (Itagaki 1969, Ackley and Itagaki 1969). Brantley and Bauer (1969) discussed the effect of charged dislocations on the dielectric constant in their piezoelectric effect study. Their calculation for an NaCl crystal, however, indicated a very small contribution ($\Delta\kappa_{22}$) to the dielectric relaxation strength κ_{22} ($\Delta\kappa_{22} \simeq 10^{-4}$ against $\kappa_{22} \simeq 6$) because of the small linear charge density (2×10^{-11} C/m) and because the quantity [(dislocation density) x (segment length)^2] for this crystallographic system is small ($\simeq 0.1$).

Since ice belongs to a different crystallographic system than NaCl with a possibly different source of the charge, the contribution of polarization of displaced dislocations to the dielectric relaxation can be considerable.

X-ray topographic observations described in this report, which constitutes the first part of a series, revealed that dislocations in ice are electrically charged, and the possible range of the magnitude was determined. Theoretical calculations of the possible contribution to dielectric polarization by charged dislocations will be discussed in the second part of this series of reports and will be based on the values obtained from X-ray topographic observation. The results will indicate that polarization due to displaced dislocations under an external electric field is sufficient to explain the well-known large audio frequency dielectric relaxation strength of ice.

The dielectric constant of dislocation-free ice between 20 Hz to 100 kHz was found to anomalously low (less than 10, Itagaki 1978). Detailed discussions will be given in the third part of this series, together with the effect of strain on the dielectric relaxation spectrum.

Reports on the effect of strain upon internal friction and other charged dislocation related phenomena such as quasi-piezoelectric effects will follow. All results supported the theory that dielectric relaxation and internal friction in the audio frequency range are caused by moving charged dislocations within the frequency range measured.

THEORY

An estimate of the charge concentration can be made if the amplitude of vibrating charged dislocations is measured under a known electric field. X-ray topography is the most promising method for making direct observations of vibrating dislocations in ice. Electron microscopy could not be used because ice would sublimate in the high vacuum. An etch pit method would

not reveal the vibrating dislocation and the etched surface would affect the movement of dislocations. The intent of the present study was to establish the charge concentration on the dislocation line by X-ray topography.

The equation of motion of a charged dislocation under a local electric field E' can be described by the following equation:

$$A\frac{\partial^2\eta}{\partial t^2}+B\frac{\partial\eta}{\partial t}-C\frac{\partial^2\eta}{\partial x^2}=E'\mu e^{i\omega t} \tag{1}$$

where $A=\pi\rho b^2$, linear mass of dislocation
η = the displacement of any point on the dislocation
B = the damping coefficient
C = the line tension
μ = the linear charge density along the dislocation
$2\pi\omega$ = frequency of applied field.

The solution under the boundary condition of $\eta(0, t) = \eta(\ell, t) = 0$ where $\eta = \eta(x, t)$ is

$$\eta=\frac{4\mu E'}{A}\sum_{n=0}^{\infty}\frac{1}{2n+1}\sin\frac{(2n+1)\pi x}{\ell}\frac{\exp[i(\omega t-\delta_n)]}{\left[\left(\omega_n^2-\omega^2\right)^2+(\omega B/A)^2\right]^{1/2}} \tag{2}$$

where ℓ = the segment length
$\omega_n=\pi(2n+1)(C/A)^{1/2}/\ell$
$\delta_n=\tan^{-1}\omega B/A\left(\omega_n^2-\omega^2\right)$.

Since the high frequency end of the present measurement ($\simeq 10^2$) is far lower than ω_0 ($\simeq 10^8$), η may be approximated by

$$\eta_{max}\simeq\pi\mu E'\ell^2/8C. \tag{3}$$

The amplitude of vibration η_{max} and the distance between pinning points ℓ can be obtained from the X-ray topograph of ice under a known applied electric field E. Local field E' can be calculated from E and the dielectric constant of κ. C is calculated from $C = 2K_s b^2/\pi$ where K_s is the energy factor for screw dislocations. The charge concentration μ is thus

$$\mu=\frac{8C\eta_{max}}{\ell^2E'} \tag{4}$$

EXPERIMENTAL APPARATUS AND PROCEDURE

Specimens used in these experiments were single crystals produced in the Mendenhall Glacier. Conductivity of molten water of the single crystals was about 5×10^{-9} S/m, indicating that the amount of ionic impurities was very low. However, minute amounts of mineral fragments were sometimes found in the meltwater. Dislocation density was about $5\times10^8/m^2$. The specimen was oriented to have a diffraction plane of $(10\bar{1}0)$ and was mounted on a holder as shown in Figure 1 with a small amount of water. It was then sliced without introducing strains by a hot wire cutter placed parallel to the (0001) plane to a thickness of about 2 mm. Both surfaces of the specimen were allowed to sublimate under a clean air stream to reduce the thickness and to provide a final finish. The final thickness was generally about 0.5 mm or less. The holder was placed in a socket on a cap and mounted on a goniometer head as shown in Figure 2. Further sublimation was prevented by sealing the cavity of the sample holder with Mylar film and by placing a small amount of crushed ice in the cavity of the goniometer with the sample. To avoid contamination, no coating was used to prevent sublimation. Gradual sublimation was unavoidable.

Due to the deterioration of sample conditions by relatively rapid sublimation compared with the time required to experiment, attempts to establish the Burgers vector of dislocations failed. Fukuda and Higashi (1969) observed that most of the dislocations in their ice samples were $1/3 < 11\bar{2}0 >$ type screw dislocations. Probably the same would apply to the dislocations observed in the experiments described here.

Lang diffraction topography was made using a Jarrell-Ash Lang camera with Norelco X-ray equipment. A sealed-off fine focus copper target tube with a nickel K_β filter was operated at 40 kV and 10 mA. Ilford L4 nuclear emulsion plates were used and developed with Kodak D-19 developer at 18°C for about 15 min. A point source port (0.4 mm x 0.84 mm) was placed about 40 cm from the specimen and an adjustable slit (3.0 mm x ≃ 10 mm) was placed 5 cm from the specimen. The vertical height of the slit was adjusted to expose the major portion of the specimen. With this configuration, reasonably sharp, high contrast topographs were obtained with relatively short exposure times (30 min). The waveforms applied to the electrode supports were 60-Hz sine waves, and 1-1/3-Hz and 1/30-Hz square waves. The field strength ranged from 300 to 60,000 V/m. These frequencies were used because the drag and mass effects on the amplitude and wave shapes of the vibrating dislocations can be

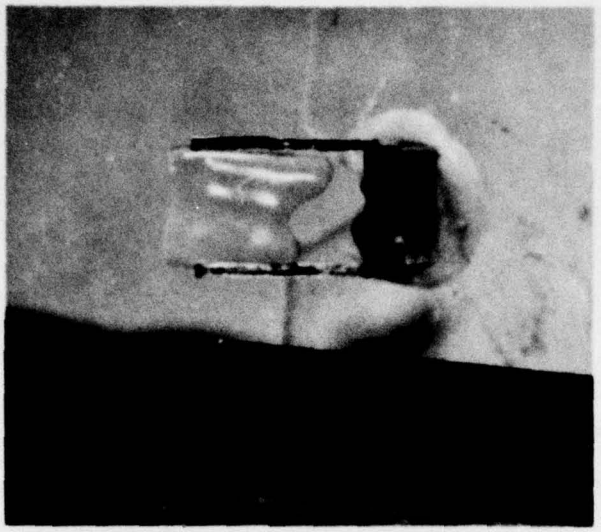

Figure 1. Ice sample mounted on the holder.

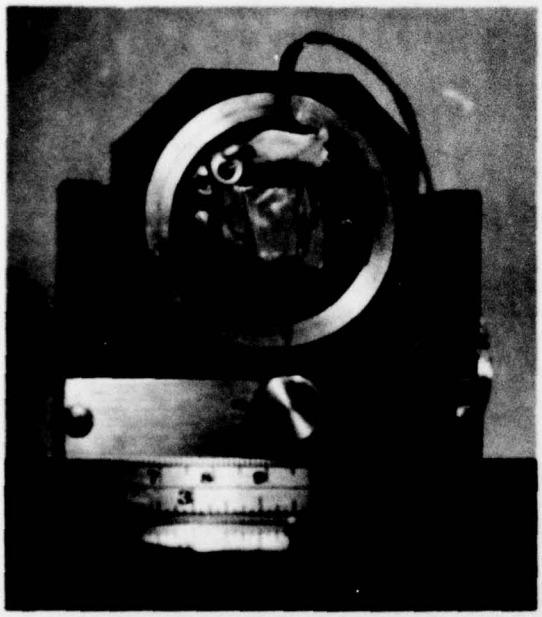

Figure 2. Ice sample on the holder installed in the goniometer cavity and electrical connections made.

considerable at higher frequencies. No observable frequency effect on η was detected within this frequency range.

The following precautions were taken to separate the dislocation motion under the electric field from the motion caused by the external mechanical and thermal forces. About one-fourth of the total exposure of a specimen was made without any electric field when the 60-Hz AC field was applied. Only boat-shaped diffused lines with a prominent center core were selected as the dislocations vibrating under the electric field (Fig. 3). Those lines were further confirmed by comparing them with the corresponding lines in topographs taken without any electric field.

Lower frequency square waves (1-1/3 Hz and 1/30 Hz) were produced by a cam-driven microswitch. A sectored lead shutter was rotated with the cam in order to reduce the exposure time during the negative cycle to one-half that of the exposure time during the positive cycle. This arrangement made it possible to distinguish the dislocations vibrating under the electric field as well as the signs of their charges (Fig. 4).

RESULTS

The measurement of length and maximum displacement η of diffused segments was required as shown in eq 4 to obtain the charge density. However, when the dislocation density was high it was difficult to make accurate measurements. A further difficulty was that the dislocation images overlapped and smeared out when the higher electric fields were applied, while the displacement under the low electric fields was limited by the resolution and was indistinguishable from motion produced by other forces. The optimum electric field was between 1,000 V/m and 5,000 V/m for individual dislocations.

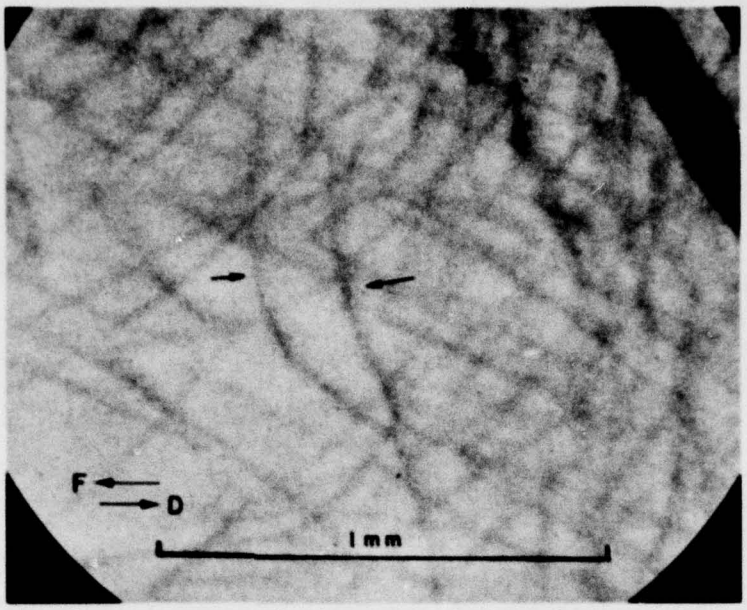

Figure 3. Dislocations under 60-Hz, 1,450-V/m AC field. Arrows indicate dislocation images with center core. (F-electric field vector, D-diffraction vector).

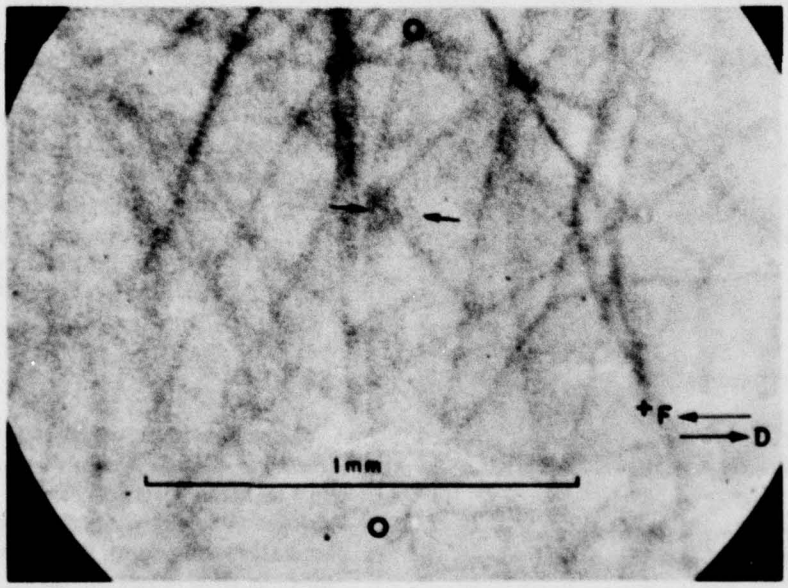

Figure 4. Boat-shaped shadow of vibrating dislocation shown between two arrows. Note left side darker than right side. Exposure during the field direction -F is one-half of that of the field direction +F. Field strength is 2,950 V/m. Frequency is 1/30-Hz square wave. Diffraction vector is D. Pinning points are the intersections of darker outlines and are indicated by open circles. η_{max} is the distance between arrows.

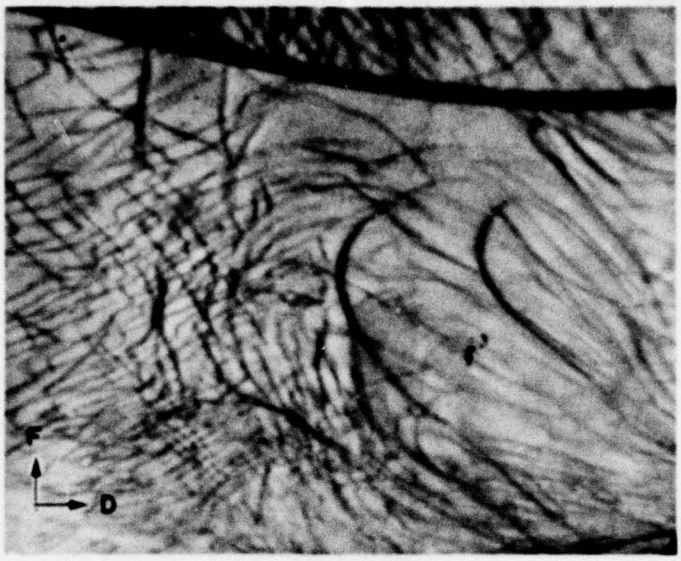

Figure 5. Straight dislocations under a high electric field that do not vibrate while curved dislocation lines show vibration (16,000 V/m, 1-1/3 Hz square wave).

Bundles of dislocations became mobile under higher electric fields in some cases (54,000 V/m). In Figure 5 straight, sharp, well-defined dislocations indicated no observable motion for field strength up to 16,000 V/m, but the curved lines were observed to have been vibrating within this range of electric field. Presumably these dislocations were trapped in the Peierls trough (see ***Discussion***). Measurements were made on only the segments which conformed to the following standards:

1. Length and amplitude of the segment could be established.
2. No motion was detected in the topographs taken without an applied field.
3. A center core was seen when the 60-Hz field was applied, or a boat-shaped shadow was darkly outlined and one side of the outline was darker than the other when the 1-1/3-Hz or 1/30-Hz square wave was applied.

Although most of the dislocations lying perpendicular to the electric field were found to vibrate under the influence of the field, only a few lines conformed to the standards mentioned above.

The measured results are shown in Table 1, columns 2 and 3. As derived from eq 3, η_{max}/ℓ^2 is proportional to the applied field (Fig. 6) although there is considerable scatter. Most of the scatter is due to difficulty in the measurement of the diffuse image.

The charge density may possibly differ according to the direction of the dislocations. Kinks may be the source of the charge of dislocations since a kink in a screw dislocation is an edge dislocation of one Burgers vector in length that has a dangling bond with it (Glen 1968). Protons on the dangling bond may be the source of charge. Density of kinks is a function of angle between the dislocation and crystallographic directions. Therefore, the charge density increases as the angle increases, if this mechanism is the source of charge.

There are several problems in estimating the local field. An assumed value for the dielectric constant does not allow accurate calculation of the local field for the following reasons:

1. The Mosotti field cannot be used for accurate calculation because it is based on a spherical cavity surrounding the dipole considered. In the present case, however, the cavity should be cylindrical with the center line in common with the dislocation line. These considerations would change the local field from $E' = E(\kappa'+2)/3$ in the spherical cavity case to $E' = E(\kappa'+1)/2$ in the cylindrical cavity case if the specimen is very thick (see Appendix A).
2. The distribution of dislocation lines is not uniform so that the local field produced by the dislocation lines and their displacement is not uniform. Also the values of the dielectric permittivity would not agree with the value used for the above calculation.
3. The specimen is thin so that the integration of the field cannot be made on an infinite volume but only on the finite slab of the specimen.

The local field acting on the cylindrical cavity can be close to the applied field under the present geometry

Table 1. Possible range of linear charge density μ for each segment measured.

Segment	Segment length $l(\times 10^{-3}$ m)	Amplitude η_{max} $(\times 10^{-3}$ m)	η_{max}/ℓ^2 $\times 10^3$/m	Sign of change	μ_{max} $\times 10^{-12}$ (C/m)	μ_{min} $\times 10^{-12}$ (C/m)
		4.75×10³ V/m 60 Hz				
1	44	6	3.1		2.2	4.8
2	60	8	2.2		1.5	3.4
3	68	8	1.7		1.2	2.6
4	60	8	2.2		1.5	3.4
5	60	4	1.1		0.8	1.7
6	60	8	2.2		1.5	3.4
7	52	6	2.2		1.5	3.4
8	100	12	1.2		0.8	1.8
9	88	6	0.8		0.6	1.2
10	80	6	0.9		0.6	1.4
11	52	8	3.0		2.1	4.6
		1.45×10³ V/m 60 Hz				
12	88	8	1.0		2.3	5.0
13	123	10	0.7		1.6	3.5
		2.95×10³ V/m 1/30 Hz				
14	128	12	0.7	+	0.8	1.7
15	116	8	0.6	+	0.7	1.5
16	48	6	2.6	+	2.9	6.4
17	64	8	2.0		2.3	5.0
Mean 75.9±26.9					1.5±0.7	3.2±1.5

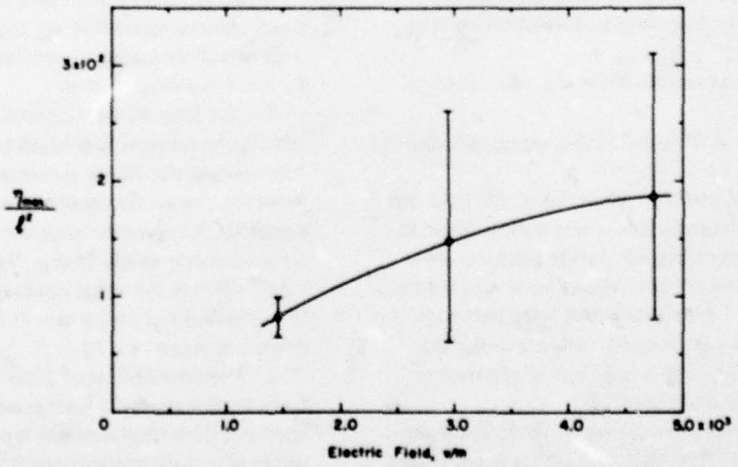

Figure 6. η_{max}/ℓ^2 vs field strength. Open circle is mean of η_{max}/ℓ^2 at the field strength and vertical bars indicate the range of measured values.

of the measurements. A potential gradient along the surface parallel to the applied field and caused by surface conduction may be the most effective source of the local field because electrodes are far apart but conducting surfaces are very close so that the contribution to the local field is stronger. Although theoretical studies on the local field were attempted, the results were inconclusive because the assumptions used were difficult to verify.

Moreover, the dielectric constants are highly dependent on the strain, presumably due to the changing dislocation structure with increasing strain, especially in the frequency range in which the present work was done. Therefore, the exact strength of the local field is in considerable doubt. The probable upper and lower limits of field strength were used in the present work and these limits defined the usable range. The upper limit of the local field which yields the lowest charge density μ_{min} (shown in the last column of Table 1) was calculated from eq 4 using the Mosotti field for a cylindrical cavity and the usually observed dielectric permittivity of unstrained ice ($\kappa' = 90$; $E' = E\,(\kappa'+1)/2 = 45.5E$). The lower limit is the external field which yields the maximum charge density μ_{max} shown in column 6, Table 1.

Only three segments were found appropriate by the above-mentioned standards to identify the sign of the charge. These charges had a positive sign. The possibility still remains that dislocation lines of negative sign can exist under certain conditions.

The results of the measurements are compiled in Table 2 for future use. Standard deviation of the distribution of (segment length)/(mean segment length) was calculated for normal and log-normal distributions. The log-normal distribution is preferred because its plot on probability paper showed better fit and also because no negative segment length was involved. However, statistical theory of the segment length pinned by a random array of point obstacles made by Labusch (1977) indicated that the shape of the segment length distribution lay between normal and log-normal distributions. The effect of segment length distribution on the observed dielectric relaxation spectrum will be discussed in the next report in this series.

DISCUSSION

There are several reports on the charge density of dislocation lines in ionic crystals. The most widely used method of measuring the charge density is based on charge generation during deformation and requires information on mobile dislocation density. If, however, some dislocations are immobilized by factors such as the charge cloud effect, the impurity effect, or the Peierls trough effect, an estimate of mobile dislocation density based on etching (which would reveal all dislocations whether mobile or not) may be an overestimate causing the charge concentration to be underestimated.

Also the Burgers vector of opposite sign could not be eliminated even if one sign dominates the other. If the electric charge of a dislocation line is not affected by the sign of the Burgers vector, opposite sign polarization will be produced by displacement of dislocations having an opposite sign Burgers vector during the deformation and would partially cancel the dominating polarization. The charge concentration obtained from charge generation, therefore, may be underestimated even further.

Zagoruiko (1965) observed motion of etch pits on a sodium chloride crystal surface under a static electric field. Several sources of error may appear when this method is used to estimate the charge concentration. For example, the local field near the surface may be affected by fringing and differ from the applied field strength; thus, the charge density μ derived from his equation ($\mu = \epsilon E/0.8K$) would affect the estimate of charge concentration. The concentration of divalent impurities required to calculate K in the same equation may be different near the surface. Also, the motion of a dislocation would be hampered near the surface, especially at the end attacked by the etchant before application of the electric field. Therefore, his equation to calculate the charge density contains several assumptions which are difficult to verify.

The present method using X-ray topography is more direct in measuring charge density on the dislocation line. However, several problems still exist which may affect the results. Possible causes which may have suppressed dislocation line motion in these experiments are the following:

1. *Surface effects*. The portions of dislocation lines which lay parallel near to the surface and which terminated on the surface seemed to have been affected by the surface. Dislocations in the thinner samples were observed to be less mobile, presumably because of this effect.

2. *Local field effects*. As the dislocation density decreased during the thinning by sublimination or by the annealing out of dislocations, the effective dielectric constant caused by moving charged dislocations may have become lower because it is directly proportional to the dislocation density (as will be discussed in Part II of this series of reports). This effect will reduce the effective field acting on the individual dislocation lines.

A lower dislocation density area is surrounded by a higher density area in Figure 7. The amplitude of

Table 2. Basic data for theoretical calculations.

a. Measured data.

Charge density	μ_{max}	$+1.5\times10^{-10}$ C/m ≃ +e/2.4*b*
	μ_{min}	$+3.2\times10^{-10}$ C/m ≃ +e/108*b*
	μ_{prob}	5×10^{-11} C/m ≃ +e/7.1*b*
Dislocation density		5×10^{9}/m^{3}
Mean segment length $\bar{\ell}$ for normal distribution		7.6×10^{-4} m
Standard deviation δ for normal distribution		0.3543
Mean segment length for log normal distribution		7.2×10^{-4} m
Standard deviation for log normal distribution		0.3367

b. Basic data for ice crystals.

Burgers vector of 1/3 < 1 1 $\bar{2}$ 0 > screw dislocations	4.5×10^{-10} m
Energy factor for the screw dislocations K_s at -10°C	3.227×10^{9} N/m^{2} *
Dislocation line tension $2b^{2}K_s/\pi$	4.16×10^{-10} N

*$K_s = (c_{44}\,c_{55})^{1/2} = (2c_{44}(c_{11}+c_{12}))^{1/2}$ (Hirth and Lothe 1968)

$c_{44} = 2.7846\times10^{9}$ N/m^{2}

$c_{11} = 13.844\times10^{9}$ N/m^{2} (calculated from Proctor 1966 for -10°C)

$c_{12} = 6.3647\times10^{9}$ N/m^{2}

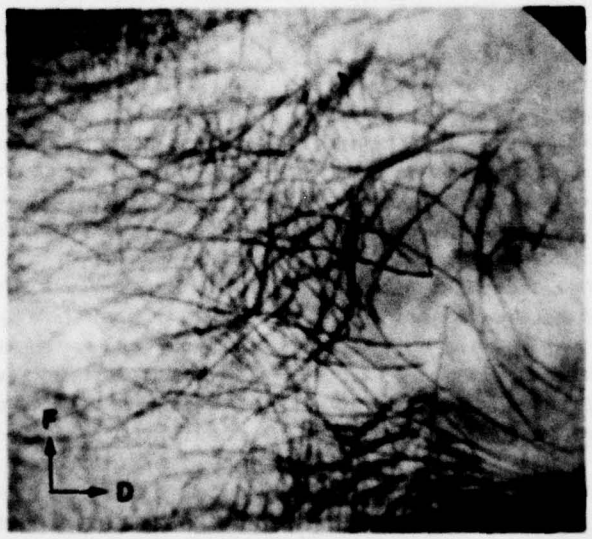

Figure 7. Vibrating dislocations in lower dislocation density area showing less amplitude than the higher dislocation density area. Field strength is 2,900 V/m at 1/30-Hz square wave.

dislocation motion in the low density area is apparently smaller than in the high density area. The smaller amplitude can be attributed to the surface or the local field effect or both.

3. *Charge cloud effects.* According to Eshelby et al. (1958), charged dislocations in alkali halide crystals are gradually surrounded by a charge cloud of opposite sign. Coulomb interaction between the charged dislocation and the slowly moving charge cloud would suppress the dislocation motion. Shielding by the charge cloud will reduce the effective field which also suppresses the dislocation motion.

4. *Impurity effects.* Various types of impurities may diffuse from the atmosphere into the ice crystals through the crystal lattice and along the dislocation lines. Although some impurities like hydrofluoric acid (HF) seem to accelerate the dislocation motion, most types of impurities would tend to constrain the motion.

It has been observed during the present experiments that the dislocation lines in newly prepared specimens are curved and mobile, while dislocations in older specimens are rather straight and immobile even under the highest electric field applied (60,000 V/m). The difference in character of the dislocations may be attributed to the charge cloud or the effect of impurities which have diffused into the older ice from the atmosphere.

5. *X-ray effects.* It is known that, in the case of alkali halides, point defects produced by X-ray irradiation at color centers pin down the dislocations (Bauer and Gordon 1962). A similar effect seems to exist in ice.

The dielectric constant of ice shows a very rapid increase followed by a gradual decrease during X-ray irradiation (Ackley and Itagaki 1971). The initial increase is presumably induced by charge carrier production, and the gradual decrease may be related to the pinning of charged dislocations by point defects produced during X-ray irradiation. Relaxation time was also reduced by X-ray irradiation, indicating the shortening of dislocation segments by pinning. The reduction of relaxation time and strength was also observed in an internal friction study supporting this notion (VanDevender and Itagaki 1973). The details of X-ray irradiation effect on dielectric and internal friction will be described in a later part of this series of reports.

6. *Troughs of the Peierls potential.* The energy of a dislocation line is minimum when it lies parallel to rows of atoms on the slip plane. This energy minimum is frequently called the Peierls trough. A dislocation which lies in the Peierls trough running along certain crystallographic orientations requires a higher energy to move out of the trough than a dislocation which does not lie in the trough. It was frequently observed that straight dislocations were generally in the $<11\bar{2}0>$ directions and were immobile (Fig. 5). Presumably the dislocations were trapped in the trough of energy minima after prolonged annealing. The X-ray topographic study on dislocation structure in ice made by Webb and Hayes (1967) showed that all Burgers vectors are of the $<11\bar{2}0>$ type. Fukuda and Higashi (1969) indicated that most of the dislocations are of the screw type. Another possibility is that the pure screw dislocation in ice may not have any electric charge as was found in some of the alkali halide crystals (Davidge 1963).

All of the above factors tend to suppress the dislocation motion. Factors 1, 3, 4 and 6 can be avoided by using thick, freshly prepared specimens. To avoid the local field effect one must observe the dislocations in the higher density regions, which makes it difficult to distinguish the pinning points of the dislocations. The X-ray effect is unavoidable in the X-ray topography method. Fortunately, this effect does not seem prohibitively strong.

A possible temperature rise produced by passing current through the specimen does not appear responsible for the dislocation vibration. The distinctive differences between Figure 8a (made with no applied field) and Figure 8b (made with a 30,000 V/m field) supports this notion. Most of the dislocation lines lying perpendicular to the electric field which appeared in Figure 8a are smeared out, of low contrast, or are spread to a boat shape in Figure 8b, while little change is observed in the lines parallel to the electric field. The vibration of dislocations due to a thermal effect would not depend on orientation.

Brantley* suggested that piezoelectric deformation is a possible mechanism to drive dislocations in the crystal. However, Tippe (1967) found no detectable piezoelectric effect in ice, and therefore this type of deformation seems unlikely. Deubner et al. (1960) found some effect which disappeared after three or four days.

A recent study on the quasi-piezo effect of strained ice single crystals (Itagaki 1978) indicated that those effects may be more easily explained by the electrically charged dislocations. If one sign of the Burgers vector charged dislocations dominates the other, a quasi-piezo effect can be produced by the displacement of the dislocations either by the mechanical stress or electrical field. The disappearance of piezoelectricity may be caused by immobilizing charged dislocations by the effects of charge clouds, impurities, or troughs in the

*W.A. Brantley, Department of Metallurgy and Material Sciences, Carnegie-Mellon University, personal communication 1969.

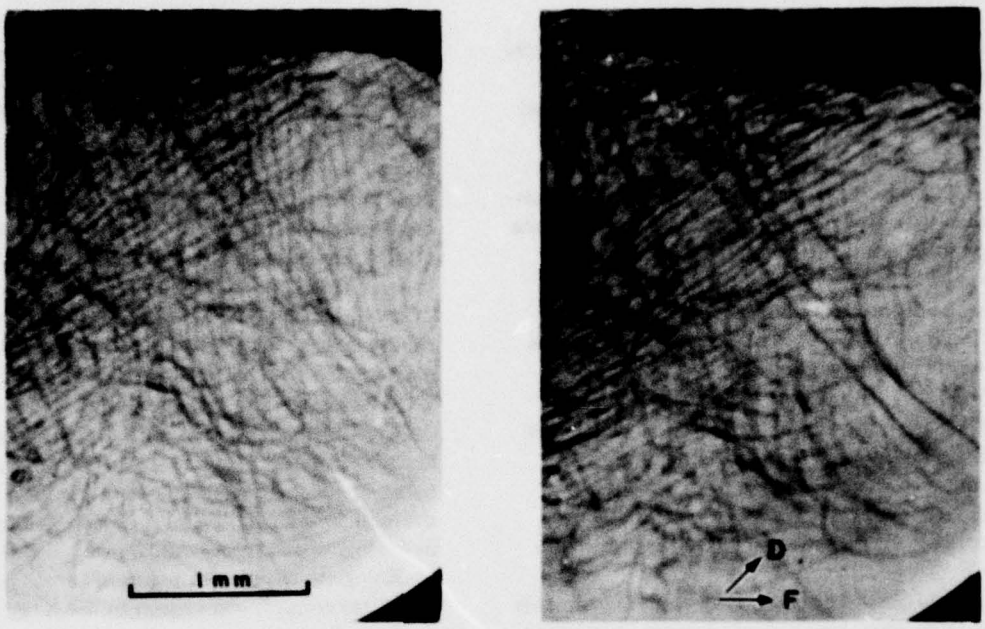

(a) (b)

Figure 8. Comparison of dislocation image without (a) and with (b) an electric field of 32,000 V/m, 1-1/3-Hz square wave.

Peierls potential as discussed previously in this report. These topics will be discussed in a later report.

CONCLUDING REMARKS

The possible range of charge density is rather wide (1.5×10^{-10} C/m to 3.2×10^{-12} C/m). However, the most probable value is 1/3 of μ_{max} because:

1. The static dielectric constant of dislocation-free ice is about 5, which is very low compared with the usually accepted value of about 100 (Itagaki 1978). This finding indicates that electrically charged dislocations are the major cause of dielectric relaxation in the audio frequency range. Assuming that the dielectric constant κ is about 5, the Mosotti field would increase the effective field E' on a dislocation line as

$$E' \approx E_{local}(\kappa+1)/2 \simeq 3\,E_{local}$$

2. The predominant contribution of surface conduction is to the E_{local} field because of the geometry of the measurements. The field produced at the electrodes would be greatly reduced by electrode polarization.

3. Most dislocation observations were made in the low dislocation density area so that there was little interference from neighboring dislocations.

Taking into account those factors E_{local} should be close to the applied field $E_{appl} = V/L$ where V is applied voltage and L is the separation of electrodes. Therefore

$$E' \cong 3V/L, \text{ and}$$

$$\mu \cong \mu_{max}/3 \cong +0.5 \times 10\text{-}10 \text{ C/m} \cong +e/7.1b$$

where b is the Burgers vector. The source of the charge is open to future studies. Several possible mechanisms have been proposed for non-ionic crystals (Glen 1968, Booyens et al. 1977).

The charge density together with the other data obtained during this study are listed in Table 2. The extent of dislocation contribution and the effects of segment length distribution on the dielectric relaxation spectra will be discussed in Part II of this series of reports.

SELECTED BIBLIOGRAPHY

Ackley, S.F. and K. Itagaki (1969) Strain effect on the dielectric properties of ice. *Bulletin of the American Physical Society* vol. 14, p. 411 (abstract).

Ackley, S.F. and K. Itagaki (1971) Effect of X-ray irradiation on the dielectric relaxation of ice. *Bulletin of the American Physical Society*, vol. 16, no. 8, p. 835.

Bauer, C.L. and R.B. Gordon (1962) Mechanism for dislocation pinning in the alkali halides. *Journal of Applied Physics*, vol. 33, p. 672-682.

Boogens, H., J.S. Vermaak and G.R. Proto (1977) Dislocations and the piezoelectric effect in III-V crystals. *Journal of Applied Physics*, vol. 48, p. 3008-3013.

Brantley, W.A. and C.L. Bauer (1969) Effect of charged dislocations on dielectric piezoelectric and elastic properties. *Journal of Materials Science and Engineering*, vol. 4, p. 29-38.

Davidge, R.W. (1963) The sign of charged dislocations in NaCl. *Philosophical Magazine* vol. 8, p. 1369-1377.

Deubner, A., R. Heise and K. Wenzel (1960) Nachweis des Piezoeffektes am Eis. *Naturwissenschaften*, vol. 47, p. 600-601.

Eshelby, J.D., C.W.A. Newey, P.L. Pratt, and A.B. Lidiard (1958) Charged dislocations and the strength of ionic crystals. *Philosophical Magazine*, vol. 3, p. 75-89.

Fukuda, A. and A. Higashi (1969) X-ray diffraction topographic studies of the deformation behavior of ice single crystals. In *Physics of ice*. (N. Riehl, B. Bullemer and H. Engerlhardt, eds.), New York: Plenum Press. p. 239-250.

Glen, J.W. (1968) The effect of hydrogen disorder on dislocation movement and plastic deformation of ice. *Physik der Kondensierten Materie*, vol. 7, p. 43-51.

Hirth and Lothe (1968) *Theory of dislocations*. New York: McGraw-Hill.

Itagaki, K. (1969) Contribution of charged dislocation motion on dielectric behavior of ice. *Bulletin of the American Physical Society*, vol. 16, no. 8, p. 835.

Itagaki, K. (1978) Dielectric properties of dislocation-free ice. *Journal of Glaciology*, vol. 21, no. 85, p. 207-217.

Labusch, R. (1977) Statistical theory of dislocation configurations in a random array of point obstacles. *Journal of Applied Physics*, vol. 48, p. 4550-4556.

Proctor, T.M., Jr. (1966) Low-temperature speed of sound in single-crystal ice. *Journal of the Acoustical Society of America*. vol. 39, p. 972-977.

Sproull, R.L. (1960) Charged dislocations in lithium fluoride. *Philosophical Magazine*, vol. 5, p. 815-831.

Tippe, A. (1967) Sum Piezoeffekt bei Eis: I. *Naturwissenschaften*, vol. 3, p. 1.

Turner, R.M. and R.W. Whitworth (1968) Movement of dislocations in sodium chloride crystals in an electric field, *Philosophical Magazine*, vol. 18, p. 531-539.

VanDevender, J.P. and K. Itagaki (1973) Internal friction of single-crystal ice. CRREL Research Report 243, AD 759930.

Webb, W.W. and C.E. Hayes (1967) Dislocations and plastic deformation of ice. *Philosophical Magazine*, vol. 16, p. 909-925.

Whitworth, R.W. (1975) Charged dislocations in ionic crystals. *Advances in Physics*, vol. 24, p. 203-304.

Whitworth, R.W., J.G. Paren and J.W. Glen (1976) The velocity of dislocation in ice-theory based on proton disorder. *Philosophical Magazine*, vol. 33, p. 409-426.

Zagoruiko, N.V. (1965) Effect of an electrostatic field and a pulsed magnetic field on the movements of dislocations in sodium chloride. *Soviet Physics-Crystallography*, vol. 10, p. 63-67.

APPENDIX A. MOSOTTI TYPE FIELD ON CORE OF CYLINDRICAL CAVITY

Let us assume a cylindrical cavity around the dislocation line as shown in Figure A1. The electrical charge ζ appearing on the surface element S of the cavity is caused by the polarization P and is given by

$$\zeta = P\cos\theta = (\kappa-1)\,\epsilon_0 E_0. \tag{A1}$$

The component of the local field in the applied field direction caused by this charge on a point A located on the dislocation line is

$$dE_2 = \frac{P\cos^2\theta\sin\psi}{4\pi\epsilon_0 R^2}. \tag{A2}$$

Since $R = \sqrt{\ell^2+r^2}$, $\sin\psi = r/\sqrt{R^2+r^2}$ and $ds = rd\ell d\theta$, then

$$dE_2 = \frac{Pr^2\cos^2\theta\, d\ell d\theta}{4\pi\epsilon_0 (\ell^2+r^2)^{3/2}}. \tag{A3}$$

The total contribution by surface integration is then

$$E_2 = \int_{-\infty}^{\infty}\int_{-\pi}^{\pi} dE_2 = \frac{P}{2\pi\epsilon_0}\int_{-\infty}^{\infty}\int_{0}^{\pi}\frac{r^2\cos^2\theta}{(\ell^2+r^2)^{3/2}}\,d\ell d\theta$$

$$= \frac{P}{2\epsilon_0} = \frac{(\kappa-1)}{2}\frac{V_0}{L}. \tag{A4}$$

The total field E' acting on the point A is then

$$E' = E_0+E_1+E_2 = \kappa\frac{V_0}{L} - (\kappa-1)\frac{V_0}{L} + \frac{\kappa-1}{2}\frac{V_0}{L}$$

$$= \frac{\kappa+1}{2}\frac{V_0}{L}. \tag{A5}$$

E_0: $(\kappa V_0/L)$ is the applied field, E_1: $((\kappa-1)V_0/L)$ is the depolarization field where the dipole contribution inside of the cavity is disregarded.

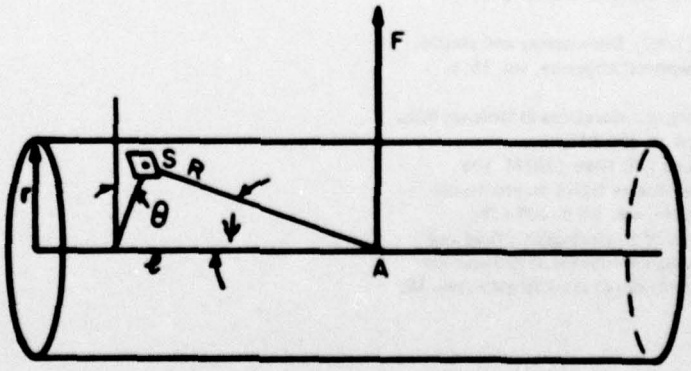

Figure A1. The charge on the surface element S of cylindrical cavity causes local field on a dislocation point A.

A facsimile catalog card in Library of Congress MARC format is reproduced below.

Itagaki, Kazuhiko
Charged dislocation in ice. I. Existence and charge density measurement by X-ray topography / by Kazuhiko Itagaki. Hanover, N.H.: U.S. Cold Regions Research and Engineering Laboratory; Springfield, Va.: available from National Technical Information Service, 1979.
iii, 12 p., illus.; 27 cm. (CRREL Report 79-25.)
Prepared for Directorate of Military Programs - Office, Chief of Engineers, by Corps of Engineers, U.S. Army Cold Regions Research and Engineering Laboratory, under DA Project 4A161102AT24.
Bibliography: p. 10.
1. Dislocations. 2. Electric charge. 3. Ice. 4. Single crystals. 5. Topography. 6. X-rays. I. United States. Army. Corps of Engineers. II. Army Cold Regions Research and Engineering Laboratory, Hanover, N.H. III. Series: CRREL Report 79-25.